# Reference Number: MEMEC-07-98

## IDENTIFICATION AND CURE FOR MORTON EFFECT VIBRATION AMPLITUDE OSCILLATIONS IN OVERHUNG COMPRESSORS

*by*: William D. Marscher and Eric J. Olson
Mechanical Solutions, Inc.
11 Apollo Drive
Whippany NJ, 07054 USA
ejo@mechsol.com

### ABSTRACT

A tilting pad bearing supported overhung compressor gradually had developed symptoms of very consistent cycling of high synchronous vibration levels. The vibration envelope cycled over a six minute period. There was a difference in the phasing of vibration increase at one end of the rotor versus the other, such that the two ends were not exactly in phase. Intensive site testing determined that no rotor critical speeds were close to the running speed of the compressor. However, it was observed with infrared thermography that the temperatures of the bearing pedestals were cyclic with the same period as the vibration, as also were the bearing pad and exit oil temperatures. The temperature cycle peaks were not in-phase with each other, nor with the vibration. Various process parameters were changed on an experimental basis, indicating that the main parametric influence was bearing oil inlet temperature. If the oil temperature was optimized in a certain range, the cycling stopped. It was concluded that the cyclic vibration behavior was a form of "Morton Effect", as discussed in recent research papers. The bearing clearances and shaft straightness were being changed by bearing oil film temperature, which in turn was being affected by vibration level, which in turn was affected by the instantaneous clearances and degree of instantaneous shaft bow. This chain of events, combined with the time lag associated with transient thermal conduction, led to the cyclic but stable oscillation of the envelope of the amplitude of synchronous vibration. During this process there was a phase angle shift of the "hot spot" which varied in a deceiving, but ultimately explainable, manner. Field testing showed that maintaining an oil inlet temperature above a practical threshold temperature minimized viscous shearing forces in the bearing film enough to prevent further thermal cycling from occurring. The ability to address the problem through a bearing design change is also discussed.

### INTRODUCTION

An integrally-geared compressor in air separation service had operated without vibration problems over the period of twenty years since it had first been installed. Passive cooling was then added to the inlet oil supply, for use when the environmental temperature was above normal. When the inlet oil was cooled in this fashion, occasionally there occurred high cyclic vibration levels of up to 2 mils p-p on this 15300 rpm pinion rotor, cycling in a sinusoidal motion over a period of several minutes. Depending upon unit load, this phenomenon could occur whenever the bearing supply temperature dropped below about 125F. The authors installed vibration probes including proximity probes near each bearing, and tri-axial accelerometers on each bearing housing, in order to observe the compressor stages during steady operation, both when the oil temperatures were high, as well as when they were at their minimum. The temperature of the oil as well as the compressor process conditions were monitored throughout the testing process. Test conditions included inlet oil temperature variations, as well as process condition variations and inlet guide vane (IGV) re-positioning for the Nitrogen as well as Air compressors.

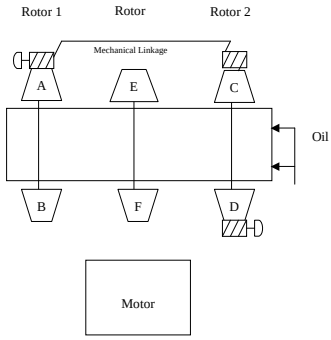
Figure 1 is a schematic of the layout of the stages of the integrally-geared compressor, shown by example in Figure 2, where the stages are arranged in pairs attached to a common high-speed pinion shaft. Each pinion shaft is driven through a flexible (gear) coupling, by a common bull gear shaft operated by a synchronous AC motor running at 1800 RPM.

### APPROACH

The authors used a 35-channel B&K Pulse FFT spectrum analyzer and digital tape recorder for the described testing. Vibration instrumentation consisted of piezoelectric triaxial accelerometers (covering three orthogonal directions) on the bearing housings, eddy current proximity probes mounted immediately next to each bearing (pinion as well as bull gear shaft), in two orthogonal radial directions, and an optically-based keyphasor that provided a tachometer signal oriented at a consistent clock position on the shaft (i.e. a keyway). Vibration frequency spectra were documented, as well as vibration amplitude versus time, phase angle (versus the keyphasor reference) versus time, and shaft orbits at each of the two bearings for the problem shaft as well as the other pinion shafts and bull gear shaft. Plant DCS RTD's, calibrated to +/- 0.5F, were used to determine bearing inlet oil temperature. An infrared pyrometer was used to determine surface temperatures of the bearing housings.

## RESULTS

As seen in the logarithmic amplitude frequency spectra of Figures 3 and 4, the vibration spectra did not show any evidence of significant subsynchronous (below running speed) vibration, or of a resonance. Both spectra are plotted with a logarithmic scale in order to emphasize the broadband vibration content. The narrowband vibration peaks at 255 Hz represent the 1x running speed vibration level. These synchronous vibration peaks contain the majority of the overall vibration content in the spectra.




| Service | Stage | Bearing | Rotor | Speed RPM |
|---|---|---|---|---|
| CP53 Nitrogen | 1 | A | 1 | 10680 |
| | 2 | B | | |
| | 3 | C | 2 | 15300 |
| CP14 Dry Air | 1 | D | | |
| | 2 | E | 3 | 25920 |
| | 3 | F | | |

| Service | Stage (Brg Pos) | Inlet Press Psia | Inlet Temp °F |
|---|---|---|---|
| CP53 Nitrogen | 3 Stage (C) | 330 | 95 |
| CP14 Dry Air | 1 Stage (D) | 280 | 95 |

**FIGURE 1: COMPRESSOR STAGE LAYOUT AND OPERATING CONDITIONS**



**FIGURE 2: EXAMPLE COMPRESSOR EXHIBITING VIBRATION OSCILLATIONS**

A broadband "mountain" peak can be seen near 195 Hz. This broadband peak represents the first bending mode of the rotor, which is sufficiently below running speed to avoid resonance. Impact testing with a calibrated hammer was used during operation, applying the authors' Time-Averaged Pulse technique [1] to determine the frequency and damping of each rotor and structural natural frequency within the range of zero to blade passing frequency. Results confirmed the logarithmic plotting of the natural excitation frequency response spectra, which in addition to not showing significant subsynchronous response or resonance, also showed no evidence of excessive aerodynamic forces, such as rotating stall, typically showing up in the spectrum as relatively broad peaks, at frequencies associated with the average motion of static pressure or velocity fields, usually at 0.3 to 0.7 times running speed.

Figures 5 through 12 show the orbits of the two compressor stages (single stage overhung wheels, on opposite sides of the same rotor, with two intervening load-between-pads tilting

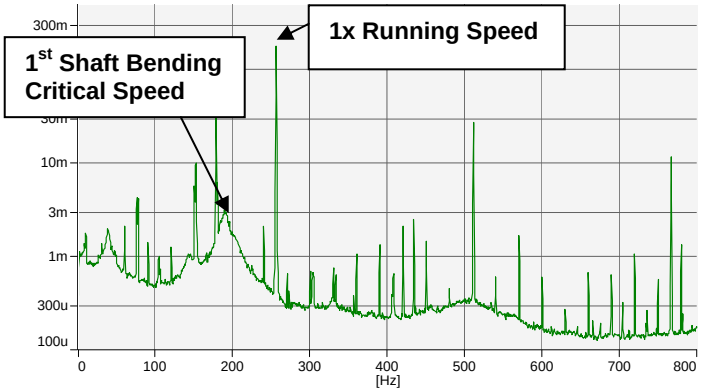



**FIGURE 3: VIBRATION SPECTRUM OF LEFT BEARING PROXIMITY PROBE (100 LINEAR AVERAGES) NOTE: RUNNING SPEED IS 255 HZ**

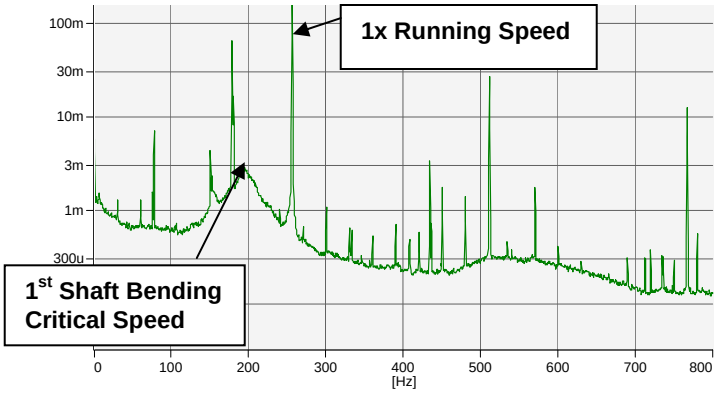



**FIGURE 4: VIBRATION SPECTRUM OF RIGHT BEARING PROXIMITY PROBE**

pad

bearings), with vibration in mils, based on the bearing orbit over one full cycle. Figure 5 shows the orbit near the peak of the cycle. Over time the orbit starts to decrease, as shown in Figures 6 and 7. In Figure 8 the orbit has reached its minimum. The orbit then begins to increase (Figures 9-11) until it reaches its maximum, as shown in Figure 12. Figure 13 shows the orbit at the same location in the cycle as Figure 5.

Vibration measured with accelerometers on the stationary casing of the machine was relatively low, and did not participate significantly in the problem vibration levels of the rotors. Therefore, the accelerometer data is not presented.

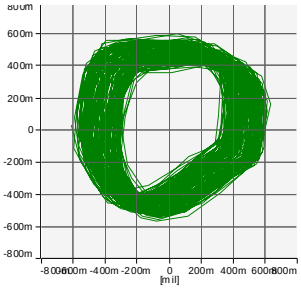



**FIGURE 5:**
**LEFT BEARING ORBIT (NEAR PEAK AMPLITUDE)**

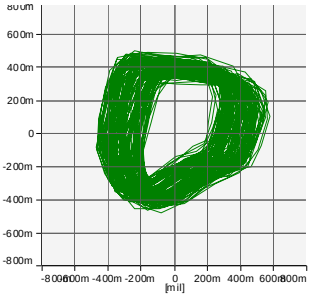



**FIGURE 6:**
**LEFT BEARING ORBIT AT 45 SEC INTO TEST**

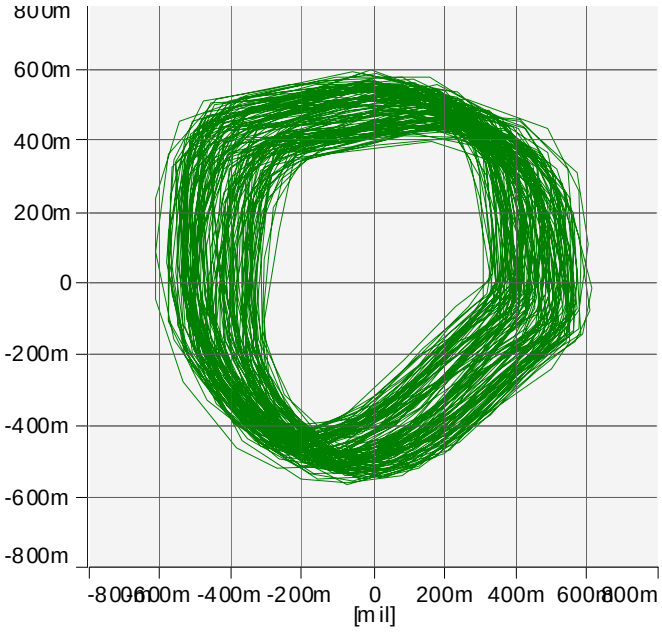



**FIGURE 13:**
**LEFT BEARING ORBIT AT 360 SEC INTO TEST**

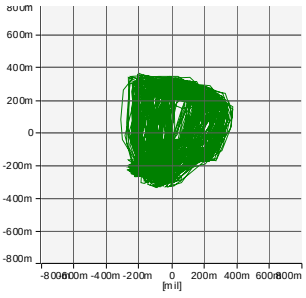



**FIGURE 7:**
**LEFT BEARING ORBIT AT 90 SEC INTO TEST**

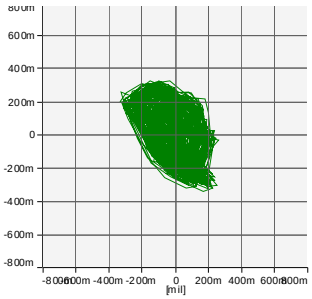



**FIGURE 8:**
**LEFT BEARING ORBIT AT 135 SEC INTO TEST**

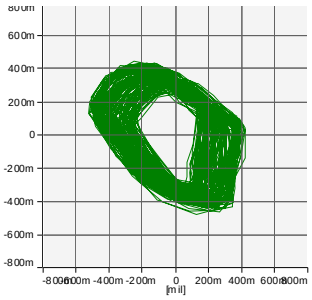



**FIGURE 9:**
**LEFT BEARING ORBIT AT 180 SEC INTO TEST**

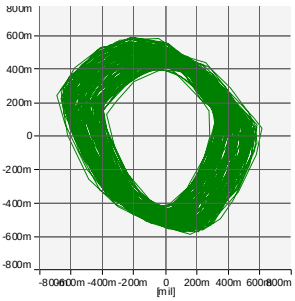



**FIGURE 10:**
**LEFT BEARING ORBIT AT 225 SEC INTO TEST**

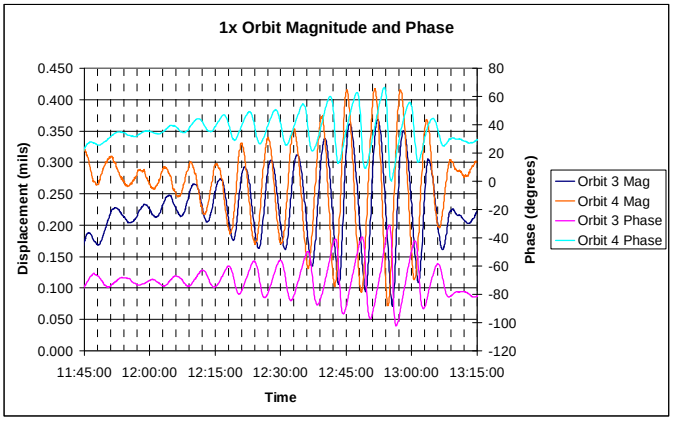



**FIGURE 14: SYNCHRONOUS VIBRATION LEVELS OF BEARINGS VS. TIME (HR:MIN:SEC)**

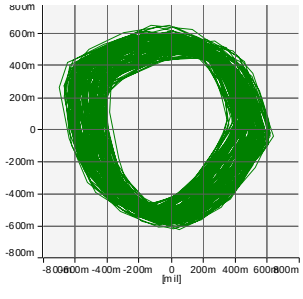



**FIGURE 11:**
**LEFT BEARING ORBIT AT 270 SEC INTO TEST**

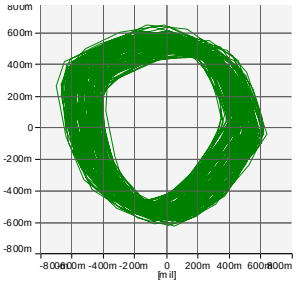



**FIGURE 12:**
**LEFT BEARING ORBIT AT 315 SEC INTO TEST**

Figure 14 compares plots of the peak amplitude of the shaft vibration envelope versus time, as well as phase angle versus the keyphasor reference location. These plots exhibit the cycling versus time, with the timing of peak amplitude occurring at different times on the opposite ends of the rotor. Note how not only the amplitude cycles, but also the phasing of the clock position of the orbit peak (i.e. farthest distance from the centerline during a revolution) versus the keyphasor position. It is this phase that is labeled "phase" or "phase angle" in Figure 14 and the following figures, which plot amplitude and phase relationships at both "Bearing 3" and well as "Bearing 4", the "inboard" (motor-side) and "outboard" bearings, respectively.

The presence of the phase cycling is important since it indicates that the net vector force acting on the rotor must be changing its phase angle with respect to the reference spot (the keyway) on the rotor circumference. The magnitude and phase information contained in Figure 14 was re-plotted as a polar plot in a form known as a "Nyquist Plot", Figure 15, where the magnitude is the radial length (from the origin) of any point in this plot, and the phase is the angle from the positive x axis to the vector. Nyquist plots are often useful for inspecting test data for natural frequencies, since the gradual increase and decrease in amplitude coincides with phase angle change as a function of frequency, such that a circle is traced out during a natural frequency crossing during compressor start-ups or shutdowns, or during modal impulse testing. In the present case, plotting the data in the Nyquist form allowed a framework for comparison of the magnitude and phase information from one data point at a time, and as will be seen, facilitated a physical interpretation of the results which confirmed the presence of Morton Effect.

## DISCUSSION

The best explanation for the gradual cycling of the synchronous vibration amplitude and phasing was the Morton Effect, which has been discussed in other applications by various investigators [2], [3], [4], and [5]. The Morton Effect is a synchronous vibration phenomenon that results from a thermal gradient imposed on the shaft within the bearing during operation, typically by close-clearance viscous shear at a consistent location on the shaft journal as it whirls synchronously. In the simplest case, the whirl occurs such that the clock position of the imbalance is identical with the instantaneous clock position of the minimum film thickness between the rotor journal and the bearing pads, due to the imbalance "forcing" the rotor against the bearing shell at this clock position. (This simplistic view is not always the case, since just above a critical speed, for example, the phase angle of the response to imbalance is between 90 and 180 degrees rather than being "in-phase" with the imbalance force). Whatever instantaneous clock position the mechanical imbalance and/ or misalignment or other forces impose on the rotor within the bore, surface heat-up occurs at that clock position, causing a thermal gradient across the shaft. The thermal growth due to the thermal gradient creates a bow in the shaft that results in thermally-induced imbalance in the direction of the clock position opposite to that of the heat-up zone, thereby relieving the original imbalance, and allowing the shaft eccentricity to decrease. This results in less viscous shear, which reduces the temperature gradient, alleviating the thermal bow. This allows the full effect of the original forcing mechanism to be present once again, allowing the cycle to take place once again. Depending upon the details of the oscillation, including the running speed location relative to the closest critical speed and mode shape "collocation" effects on the thermal bow axial location versus the axial location of the imbalance (i.e. does a mode shape "crossing" take place between the two, causing a 180 degree phase shift), the thermal bow amplitude effect on the vibration may increase as well as decrease the vibration, depending upon the instantaneous phase angle of the thermal bow versus the original mechanical force (e.g. imbalance) phase angle. In fact, if the thermal and mechanical phase angles are other than zero or 180 degrees with respect to each other, the "pinch" clock position of the bearing continuously changes as the thermal bow vector interacts with the mechanical force vector. This effect is clarified by reference to the Nyquist plots drawn for the subject compressor, beginning with Fig. 15.

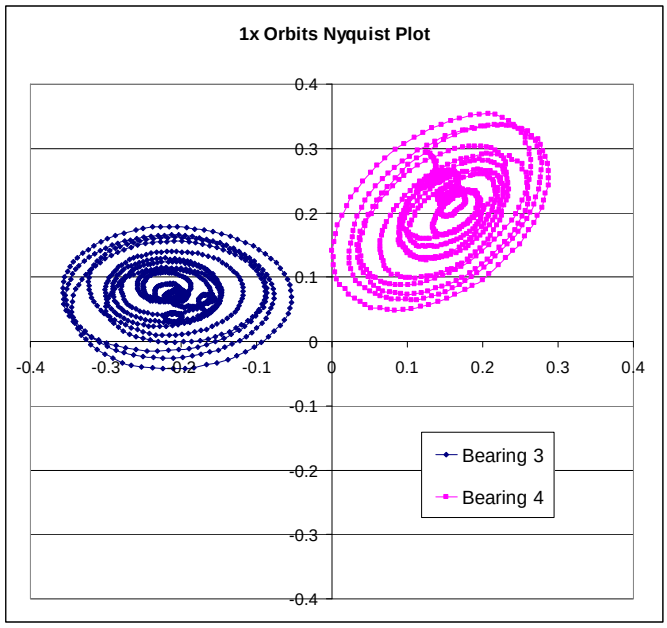



**FIGURE 15: NYQUIST PLOTS OF ORBIT SIZE & PHASE LEFT ("BEARING 3") AND RIGHT ("BEARING 4") ORBITS**

The Nyquist polar plot in Figure 15 shows the consistent cycling over time of the magnitude and phase of the two bearing orbits. Note that these plots are NOT the orbits themselves, but are polar plots of the orbit size vs. rotor phase angle, with each dot representing a subsequent revolution of the shaft. The magnitude and phase of the orbits cycled in a manner that suggested that the overall cyclic thermal vector force on the rotor acted over a full 360 degrees through one complete cycle, resulting in a net thermal + mechanical combined vector phase change of only 60 degrees or so, which was misleading. The epicenter of the full-circle

oscillation in this plot is offset from zero, and is located vectorially at a location of the plot that represents the amount of original imbalance response, and the angular location of this response relative to the keyphasor. There is a separate epicenter for each bearing, because the amount and location of the original imbalance on each impeller wheel (one at each opposite end of the rotor) is different.

Figures 16 through 17 provide plots similar to Figures 14 and 15, but exhibit the details of the cycling in the two orthogonal directions perpendicular to the shaft at each of the two bearings. Notice how the peaks and valleys of the cycling of the "x" versus "y" direction of a given bearing coincide with each other in time, both with regard to the amplitude envelope magnitude oscillation as well as the phase oscillation. This indicated that a critical speed was not involved, since then the two directions would be expected to behave differently in both amplitude growth timing as well as phase change timing, as first one direction of a rotor mode and then (at a somewhat different frequency) the orthogonal similar mode would be tuned in.

To make the thermal versus mechanical vector superposition effects clear, Figure 18 shows the residual mechanical imbalance vectors and the apparent cyclic thermal imbalance vectors overlaid on the Nyquist plot. This experimental plot clearly shows that the cyclic thermal vectors (whose action is centered on the original mechanical vector tip) are acting over a full 360 degrees during one complete cycle. The Nyquist plot shows however that the net global phase angle change taken up by the two orbits is deceptively only approximately 60 degrees, mis-directing previous troubleshooters to look for causes other than Morton Effect.

Figure 19 shows the extreme net force vectors for the two orbits and the phase angle between them. The location of the temperature gradient will depend on the phase angle of the net force vector (i.e. the sum of the thermal and the mechanical imbalance vector). Therefore, the phase angle of the thermal imbalance will cycle with the phase angle of the net force vector. The test data shows that the combined thermal imbalance from both ends cycle 360 degrees. Note that the cycling of the two ends can be resolved into vectors such that at least part of the thermal imbalances are 90 degrees out of phase, and therefore the locations of the individual thermal imbalances have a phase angle between them, as would also be the typical case (i.e. it would be an unusual coincidence for both rotor ends to have their residual imbalance and/ or bow in the same circumferential location). In this instance, this mechanism can explain the cyclic behavior, where orthogonal response allow real & imaginary interaction between the cyclic force and cyclic response, encouraging the sinusoidal cyclic behavior of the Morton Effect.

When the problem thermal gradient is initiated by viscous energy dissipation in the bearings, then as oil temperature is decreased this viscous shear energy increases, causing increased local temperature and increased thermal bow. In the case of the tested rotor it was surmised that, once the oil temperature dropped below approximately 125F, the thermally-induced imbalance became large enough to compete with the residual mechanical imbalance in this manner. This changed the angular location of heat input, the direction and amount of the net bow, and therefore the level and phasing of peak vibration response, initiating vibration amplitude cycling. A superior long-term solution would be a bearing re-design, less susceptible to shaft hot-spot formation. Shafts with thermally-insulating bearing journal sleeves, or internals designed using the criteria of Kirk [5] could accomplish this purpose.

At oil inlet temperatures above 128 F, the viscous shearing forces were small enough that they did not create a large enough thermal imbalance to lead to cycling. Below 128 F, the shearing forces increased to the point that an oscillation threshold was reached, as predicted by Kirk et al [5], and at least some degree of cycling was seen. Once the temperature was brought back above 128 F, the thermal cycling ended and the vibration levels remained steady and moderate.

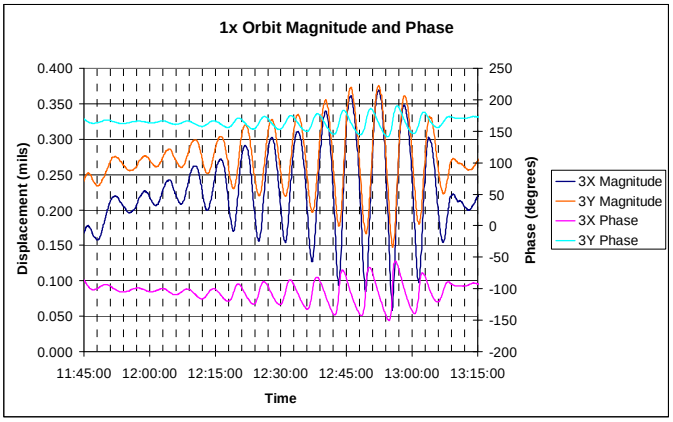



**FIGURE 16: SYNCHRONOUS VIBRATION LEVELS OF PROBES 3X AND 3Y DURING TESTING**

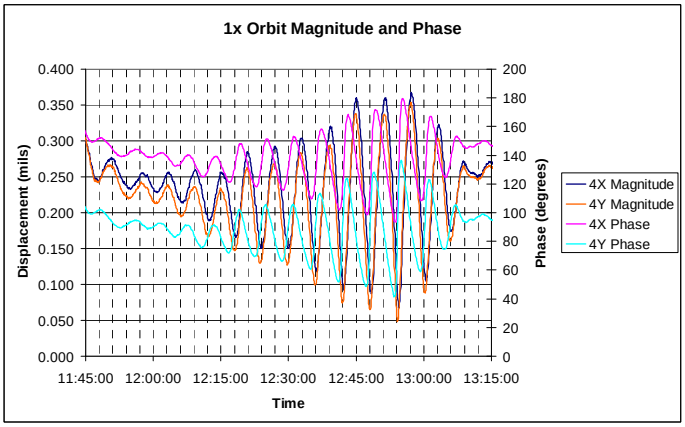



**FIGURE 17: SYNCHRONOUS VIBRATION LEVELS OF PROBES 4X AND 4Y DURING TESTING**

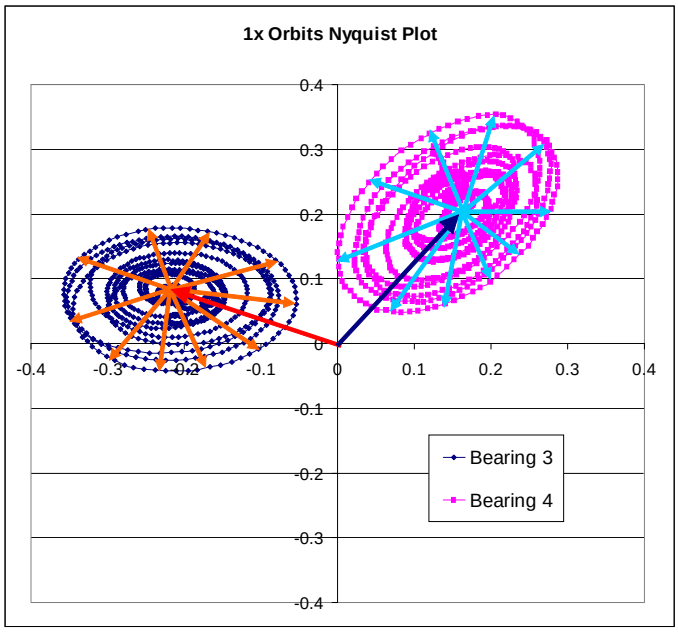



**Figure 18: NYQUIST PLOTS OF ORBITS WITH RESIDUAL MECHANICAL IMBALANCE AND CYCLIC THERMAL IMBALANCE VECTORS OVERLAID**

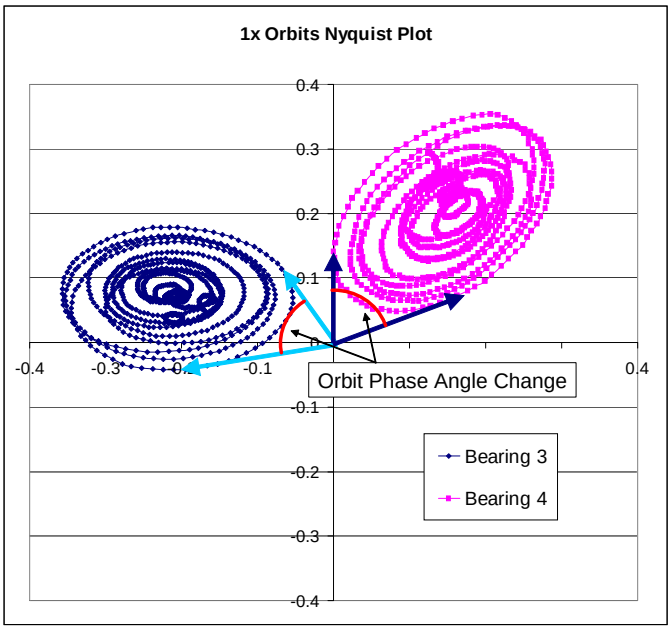



**FIGURE 19: NYQUIST PLOTS OF ORBITS 3 AND 4 WITH NET IMBALANCE FORCE VECTORS OVERLAID**

## CONCLUSIONS

1. When oil inlet temperature was below a threshold level of 125F, the envelope of vibration of the rotor was observed to cycle to excessive levels according to a consistent period of about 6 minutes.
2. Increasing oil inlet temperature above 128F effectively eliminated the high vibration and long period cycling. Analysis indicated that an appropriate bearing design less prone to local hot spots would also have been an effective solution.
3. The vibration was synchronous with no evidence of resonance or subsynchronous instability.
4. If the problem was due solely to an imbalance, it would not be expected to slowly cycle, and the vibration of each stage of the rotor would be expected to increase or decrease in phase end-to-end, unlike the present case.
5. Newkirk Effect (rotor rubbing, heating, wearing, cooling, and thereby reversing imbalance location on a cyclic basis) could possibly explain the cyclic behavior, but the associated rapid wear of the rotor did not occur.
6. "Morton Effect" is a form of imbalance or shaft bow which changes its magnitude and phasing on a cyclic basis. This appears to have been the source of high cyclic vibration since it is the only theory consistent with all data.

## REFERENCES


1. Marscher, W, *The Determination of Rotor Critical Speeds While Machinery Remains Operating through Time-Averaged Pulse Impact Testing*, IMAC Conf. Orlando FL, SEM, Feb. 1999
2. De Jonge, F.M., and Morton, P.G., 1994, *The Synchronous Instability of a Compressor Rotor Due to Bearing Journal Differential Heating*, ASME Paper 94-GT-35, pp. 1-13.
3. Keogh, P.S., and Morton, P.G., 1994, *The Dynamic Nature of Rotor Thermal Bending Due to Unsteady Lubricant Shearing Within Bearing*, Proc. Royal Soc. of London, Series A, n. 445, pp. 273-290.
4. Faulkner, H.B., Strong, W.F., Kirk, R.G., 1997, *Thermally Induced Synchronous Instability of a Radial Inflow Overhung Turbine*, DETC97/VIB-4063, Proc. ASME Design Engineering Technical Conf, Sept. 14-17, 1997, Sacramento CA.
5. Kirk, R.G., Guo, Z., Balbahadur, A.C., *Synchronous Thermal Instability Prediction for Overhung Rotors*, Proc. 22nd Texas A&M Turbo Symp., Sept. 2003